

# Nonlinear Switching Control of Bipedal Walking Robots with Provable Stability

Jianjuen Hu and Gill Pratt

Artificial Intelligence Laboratory, MIT  
Cambridge, MA 02139, USA  
{ kjh, gill }@ai.mit.edu  
<http://www.leglab.ai.mit.edu/>

**Abstract** A new approach is proposed to achieve provably stable locomotion control for a bipedal walking robot. This approach applies nonlinear switching control theory in the locomotion control system so as to ensure bipedal gait stability in the stable limit cycle sense. The switching surface is determined by means of the orbital contraction tuning technique and Zero-Moment-Point (ZMP) computation. Both postural and gait stability are analyzed in the paper.

One implementation of this switching control technique is proposed and verified by computer simulation. Simulation results are reported and discussed in the paper.

## 1 Introduction

Whether it is rigorously proven or merely observed, stability is a critical requirement in the control of bipedal walking [1,4]. But unlike conventional control system stability, a walking robot's stability is not a question of tracking desired trajectories [14]. To realize walking, a biped should not fall down and should walk at a steady pace. In other words, its posture (roll, pitch, yaw, height) should be bounded within some range of nominal values, and its gait should converge to a periodic orbit. We denote these two ideas as *Postural Stability*, and *Gait Stability*.

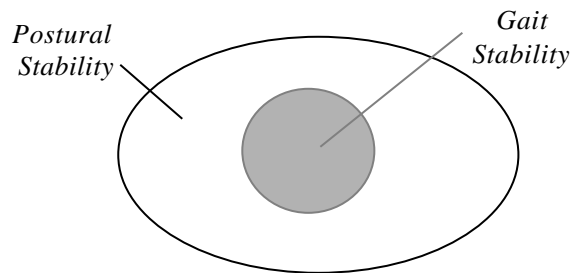


**Figure 1:** Description of relationship between gait stability and postural stability of a walking robot.

Figure 1 shows the relationship of gait stability and postural stability. Note that a robot may have postural stability, and not have gait stability – for example its leg motion might be aperiodic or even chaotic [17] - but not the other way around. Ideal walking requires both gait stability and postural stability.

Many researchers have previously studied postural stability. Recently, Zero Moment Point (ZMP) has become a common criterion for achieving postural stability, as with the Honda humanoid robots [2] and the WABIAN robots [3] etc.

Gait stability has been much less studied. A few researchers have addressed this topic in passive walking [7,9] and running [17], and some neural models [5,6]. McGeer (1990), a pioneer in passive bipedal walking [9], demonstrated that a passive walker can attain a stable periodic motion, and he analyzed this behavior with a linearized mathematical model. Recently, Goswami et al (1996) studied the periodic behavior of a passive compass gait of a biped [7]. With neural oscillators one can generate a nonlinear limit cycle process to accomplish bipedal walking [5]. Taga (1995) addressed this in his neural oscillator driven humanoid-legged locomotion control [6].

But the majority of studies on gait control have focused on gait modification and implementation for different terrain [2] instead of stability. Despite this lack of work, gait stability is crucial for locomotion. Without gait stability, the leg motion and forces available to the robot to maintain postural stability become unpredictable, and postural control may fail despite a good postural control method.

In his study of stability, Vukobratovic proposed a repeatability condition [1], which is required for the stability of a periodic gait. In this paper, an active locomotion control approach is proposed by means of nonlinear switching control schemes that meet this condition. It can be used to achieve postural stability and gait stability. In this approach, we used different controllers for the double support and single support phases. The ZMP computation and an orbital contraction tuning technique are used to choose the state-dependent switching surfaces. Nonlinear control theory is then used to prove gait stability.

The second section of this paper addresses the overall system structure of our control system. The stability of this method is discussed in section 3. Section 4 introduces the switching control. In section 5, gait stability is analyzed by means of nonlinear contraction theory. Simulation results are reported at the end of the paper.

## **2 Overall Control System Structure**

### **2.1 Overall Control of System Structure**

Figure 2a shows the overall control system. There are five main components: a state machine, ZMP computation module, state observer, control sub-systems and a switching control module. The control sub-systems are provided for different walking phases (single support, double support). The transition from one controller to another controller during walking is determined by the switching control module, which is based on the state machine, the real time ZMP computation module and orbital gait contraction tuning.

The structural dynamics of a bipedal robot change with the different phases of a walking cycle. The dynamics are different between single support states (left single support, right single support) and double support states. Consequently, the corresponding controllers should change with respect to the states. A complete walking

cycle can be broken down into five states, left single support I, left single support II, double support, right single support I, and right single support II.

We design control sub-systems for each state, and then switch them from one sub-system to another by observing the overall system state variables [4,10]. In our control system (Figure 2a), the switching control is on top of control sub-systems and supervises the control sub-systems. Figure 2b describes a state machine for five walking states and their transitions.

Single support I is the walking phase during which the swing leg leaves the ground and starts swinging forward until the swing leg passes over ankle point of the stance leg.

Single support II state specifies the rest of swing phase when the swing leg swings from the ankle position of the stance leg until it strikes the ground.

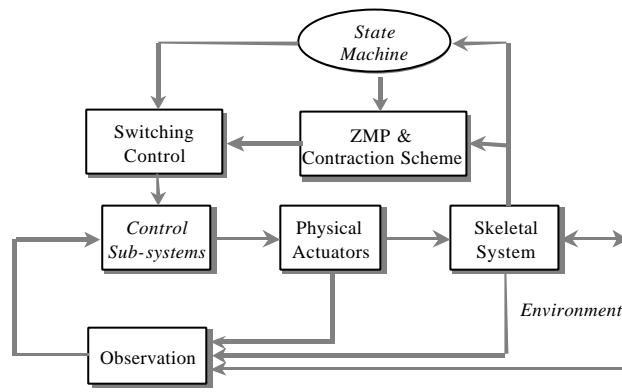


**Figure 2a:** System structure of the switching control

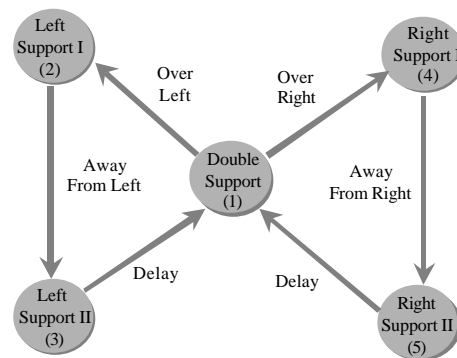


**Figure 2b:** Diagram of state machine.

## 2.2 Dynamics Models and Control Sub-systems

Approximate dynamics models are used in our controller design of each sub-system. We assume that the dynamics in the sagittal plane and forward plane are weakly coupled, and hence the controller design can be done separately for 3-dimensional bipeds [14].

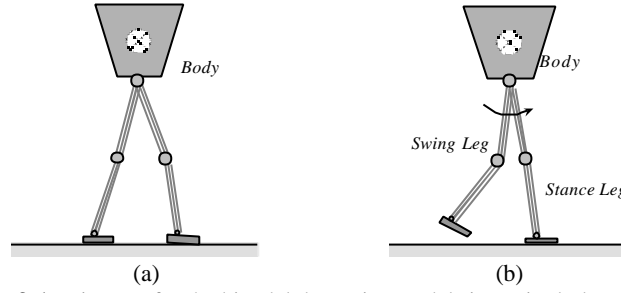


**Figure 3-1:** Diagram for the bipedal dynamics models in sagittal plane: (a) double support, (b) single support.

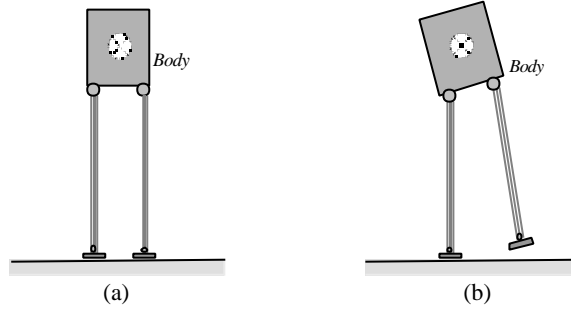


**Figure 3-2:** Diagram for dynamics models in lateral plane: (a) double support, (b) single support.

In double support (see Figure 3-1(a) and Figure 3-2(a)), the structural dynamics are stable and controllable within the range of dynamic constraints. The redundant degrees of freedom in the double support state provide us more room for control. We can control the robot trajectories by conventional control techniques [11], or we can use a virtual model control approach [10] in dealing with the structural redundancy.

In the single support state (see Figure 3-1(b) and Figure 3-2(b)), the dynamics are unstable. The stance leg cannot be controlled completely, but it can be treated as a double inverted pendulum rotating with respect to the ankle joint of the stance leg. The swing leg is controllable as a regular pendulum. The control approaches developed for manipulators can be applied.

Generally, the dynamics for a biped can be formulated as

$$M(\mathbf{q})\ddot{\mathbf{q}} + N(\mathbf{q}, \dot{\mathbf{q}})\dot{\mathbf{q}} + G(\mathbf{q}) = \mathbf{u} \quad (1)$$

where  $M(\mathbf{q})$  is the inertia matrix,  $N(\mathbf{q}, \dot{\mathbf{q}})$  is a matrix with the Coriolis and centrifugal coefficients,  $G(\mathbf{q})$  is a vector of gravitational torques,  $\mathbf{q}$  is the state variable, and  $u$  is the torque commands.

The above formula holds for the dynamics in the single support phase of both the sagittal plane and frontal plane except that the matrices are different. Based on the above formula, the characteristics of the sub-systems can be analyzed. With further manipulations of the dynamics, nonlinear feedback control and linearization based control theories can be applied [12,13].

### 3 Stability

Postural stability can be specified in terms of an index like body pitch angle, roll angle and height. Figure 4 shows the postural stability with a height index. The ZMP criterion is usually utilized for monitoring postural stability [1,3], and it can also be used to specify the stability boundary.

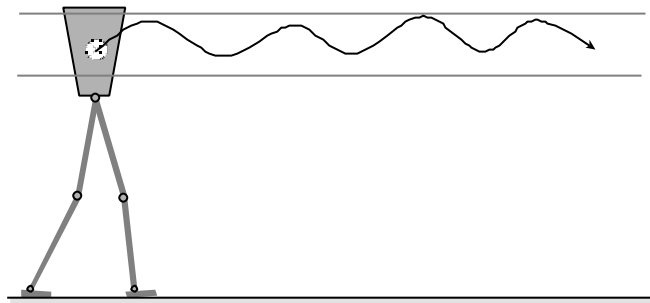


**Figure 4:** Postural stability with height index.

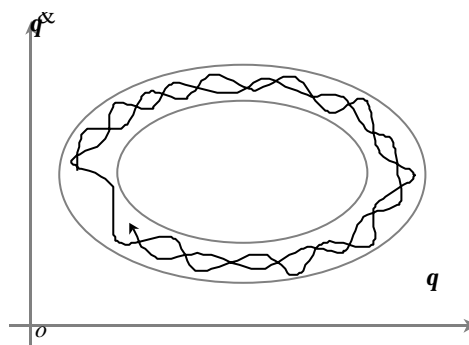


**Figure 5:** A description of approximate cyclic motions, which are confined a very narrow region. When the volume of the region shrinks to zero, a perfect limit cycle is achieved.

Gait stability requires a globally stable cyclic motion of the robot. That is, the global motion should be periodic. From Vukobratovic's definition [1], this implies that all the states and velocities should be repeated with a constant period and stride length. In this study, we create a global index variable that abstracts the state of the legs, and enforce stability on this variable and its derivative to satisfy the repeatability condition. In the phase plane presentation, the behavior of a biped joint should be confined within a certain range of orbit (Figure 5).

## 4 Switching Control

From human and bipedal animals' walking, we observe that combining double support phases (controllable and stable dynamics) and single support phases (uncontrollable and unstable dynamics) can yield stable periodic bipedal walking. In this section we will show how a suitable switching control technique can combine stable double support and unstable single support subsystems to produce stable periodic motion, even at high speeds where the double support phase becomes very short.

### 4.1 Characteristics of steady gaits in phase plane

As shown in Figure 6,  $\mathbf{f}$  is the global index variable we create. It refers to the angular position of a leg measured from the line connecting the ankle and the hip of the leg to a vertical axis. There are two global variables,  $\mathbf{f}_l$  and  $\mathbf{f}_r$ , for the left leg and right leg respectively. Given that the bipedal robot has symmetric structure, we assume that the dynamics for the global variables  $\mathbf{f}_l$  and  $\mathbf{f}_r$  are also symmetric.

With this global variable  $\mathbf{f}$ , the characteristic of steady gait behavior can be viewed in the phase plane clearly. In Figure 7, a phase portrait of one complete walking cycle (for one leg) is shown. Since the two legs of a biped are symmetric, this phase portrait describes the motion of each leg. In the phase plane, we only refer to the global variable for the left leg. As shown in Figure 7, there are only four phases defined in a walking cycle: double support with the left leg leading, single support with the left leg supporting, double support with the left leg behind and single support with the left leg swinging.

The switching control model decides the switching points in the phase plane,  $t_i$ ,  $i = 0,1,2,3,4$ . At  $t_4^-$ , the leg strikes on the ground, then the angular velocity jumps from  $t_4^-$  to  $t_4^+$  ( $t_0 = t_4^+$ ). In Figure 7, at time  $t_0$ ,  $t_2$ , when the swing leg strikes the ground, the control mode switching is immediately enforced. The switching points  $t_1$  and  $t_3$  can be appropriately selected by the switching control schemes (described in the following section). Two different types of switching control are used in this study: ZMP computation based switching and contraction theory based switching.

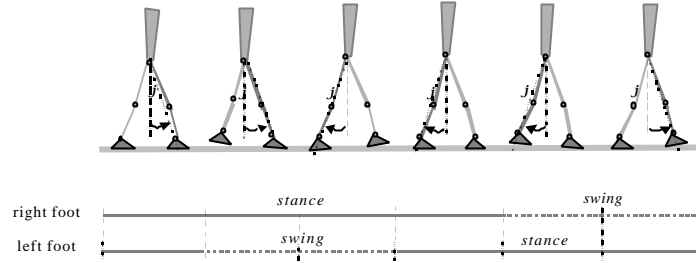


**Figure 6:** Diagram describing the global variable  $f$  defined with respect to the right leg (dark shading).

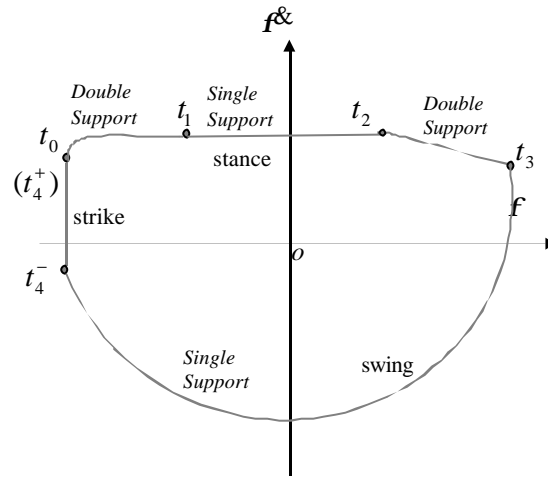


**Figure 7:** Switching control in phase plane of global variable  $f$ . There are four switching points in this phase portrait:  $t_0$ ,  $t_1$ ,  $t_2$  and  $t_3$ , where  $t_4 = t_0$ .

## 4.2 ZMP Computation based switching control

### 4.2.1 ZMP computation

We now discuss the ZMP computation in 3-D for the 7-link biped model in Figure 8. By applying D'Alembert's Principle, the equation of motion at a fixed point  $P$ , which is defined as a ZMP, is formulated as

$$\sum_{i=1}^7 m_i (\ddot{r}_i - \ddot{p}) \times (\ddot{r}_i + g) + \sum_{i=1}^7 H_{gi} + T_m = 0 \quad (2)$$

where  $m_i$  is the mass of the  $i$ th link;  $\mathbf{p}_i = [x_i, y_i, z_i]$  is the position vector of the  $i$ th link at its COM;  $\mathbf{p} = [x_p, y_p, z_p]$  is the position vector of point  $P$ ;  $\mathbf{g} = [g_x, g_y, g_z]$  is the gravitation acceleration;  $T_m = [T_x, T_y, T_z] = [0, 0, *]$  is the total torque computed at point  $P$ ;  $H_{gi}$  is the angular momentum about the COM of the  $i$ th link. Then from equation (2), we can determine the ZMP location on the ground point  $P$ :

$$x_{zmp} = \frac{\sum_{i=1}^7 m_i (g_y + g_z) x_i - \sum_{i=1}^7 m_i (g_x + g_z) z_i - \sum_{i=1}^7 H_{gix}}{\sum_{i=1}^7 m_i (g_y + g_z)} \quad (3)$$

$$y_{zmp} = \frac{\sum_{i=1}^7 m_i (g_x + g_z) y_i - \sum_{i=1}^7 m_i (g_x + g_y) z_i - \sum_{i=1}^7 H_{giy}}{\sum_{i=1}^7 m_i (g_x + g_z)} \quad (4)$$

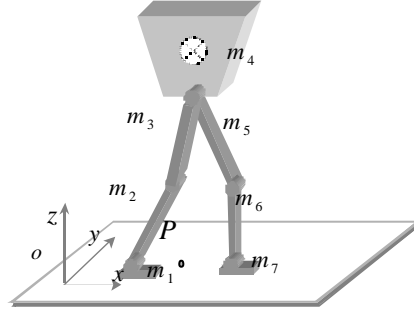


**Figure 8:** Diagram for ZMP computation. Point  $P$  is the ZMP of a 7 link biped.

#### 4.2.2 ZMP based switching control

When the ZMP is within the region shown in Figure 9, the biped is stable in double support, which means that postural stability is achieved. If the robot starts to fall down in double support, it is very difficult to recover the stability in the following single support phase since the dynamics in the single support phase are unstable and uncontrollable; and the failure of postural stability in the previous double support phase will also affect the global gait stability. In this case, switching control becomes very important. With an uncontrollable single support phase and a fully controllable double support phase alternatively switched on, we can achieve a stable walking gait.

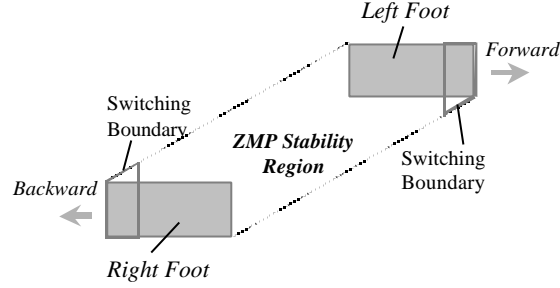


**Figure 9:** Diagram for local postural stability. The outside polygon specifies the ZMP stability region in double support phase. The two trapezoids (at the heel of right foot and at the toe of the left foot) are switching zones.

To guarantee stability in the double support phase, the ZMP has to stay in the polygon area (Figure 9). Whenever the ZMP approaches the boundary line of the polygon area, the switching action is forced. Switching is also allowed while the ZMP is in the polygon area for the purpose of gait stability.

### 4.3 Switching control with contraction tuning

Gait stability can be reached by appropriately switching between single support phases and double support phases. The switching point can be adjusted in the boundary area (Figure 9) in order to balance the kinetic energy and the potential energy in the single support phase. The goal is to enforce the repeatability condition (gait stability), while the constant stride length (step length) is guaranteed by means of controlling the swing leg. The repeatability condition with symmetry is expressed as:

$$\dot{x}_l(t_0) = \dot{x}_r(t_0 + T) \quad (5)$$

$$\dot{x}_r(t_0) = \dot{x}_l(t_0 + T) \quad (6)$$

$$\ddot{x}_l(t_0) = \ddot{x}_r(t_0 + T) \quad (7)$$

$$\ddot{x}_r(t_0) = \ddot{x}_l(t_0 + T) \quad (8)$$

where  $t_0$  is the previous touch down time instant of a foot,  $T$  is the period of one step, and  $\dot{x}_l$ ,  $\dot{x}_r$  are the state variables for the left leg and right leg respectively.

Khalil's definition of orbital stability [8] is used in this section. We consider a general continuous nonlinear system,  $\dot{\bar{x}} = f(\bar{x}; t)$ . One can analyze the system trajectory in the vector space of  $\bar{x}$ . The phase trajectory  $L$  of this system is orbitally stable if, given  $\epsilon > 0$ , there is  $\delta > 0$  such that, if  $R$  is a representative point (on another trajectory  $L$ ), which is within a distance  $\delta$  of  $L$  at time  $t_0$ , then  $R$  remains within a distance  $\epsilon$  of  $L$  for  $t > t_0$ . If no such  $\delta$  exists,  $L$  is orbitally unstable. Analogous to the asymptotic system stability of the conventional control system theory, we may say that if the trajectory  $L$  is orbitally stable and, in addition, the distance

between  $R$  and  $L$  tends to zero as time goes to infinity, the trajectory  $L$  is asymptotically orbitally stable.

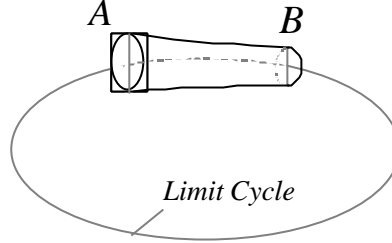


**Figure 10:** An illustration of contraction in  $\overline{AB}$ .

For a walking cycle of a biped (Figure 5), we consider a piece of dynamic orbit  $\overline{AB}$  in the  $k^{th}$  cycle between positions  $\mathbf{f}_A$  and  $\mathbf{f}_B$ . In the phase plane, let

$$y_k = \mathbf{f}(\mathbf{f}_k^B) = F(\mathbf{f}_k^B) \quad (9)$$

$$x_k = \mathbf{f}(\mathbf{f}_k^A) = F(\mathbf{f}_k^A). \quad (10)$$

If the following inequality is satisfied,

$$\begin{aligned} |y_{k+1} - y_k| &= |F(\mathbf{f}_{k+1}^B) - F(\mathbf{f}_k^B)| \\ &\leq c \cdot |x_{k+1} - x_k|, \end{aligned} \quad (11)$$

where  $0 < c < 1$ , then the orbit session  $\overline{AB}$  is called in contraction. For the entire orbit, we can similarly prove the volume contraction one session after another.

There are a few ways to achieve the above contraction behavior in a dynamic system. One way is to adjust the boundary condition of the system; the other is to change the system's dynamic structure. In this paper, we choose to use the former method.

#### 4.4 Robustness with switching based locomotion control

With the above approach, the local postural stability under disturbances can also be achieved in double support phase [4,10]. The vertical ( $Z$ ) and pitch ( $q$ ) disturbances can be rejected with the control sub-systems in either the double support or single support phases. But the disturbances in the forward ( $X$ ) direction cannot be taken care of with the control sub-systems [4]. However, the switching control can maintain local postural stability:

- a) When disturbances are exerted along the  $X$  axis in the double support, they can be rejected in the current double support phase if the double support phase is long enough. Otherwise, the switching control will take care of them by executing an advanced or a delayed switching point. If the disturbances are very big in double support, the switching control will command a foot to step forward or backward.

- b) When disturbances are exerted in  $X$  axis in single support phase, the controller in the next double support phase and the contraction tuning based switching control can stabilize it.

## 5 Gait Stability with Switching Control

If the behaviors of the global variables approach limit cycles, then we induce that the behaviors of any joint variables are confined in the neighborhood of limit cycles. In our gait stability analysis, lateral control stability is assumed for a simplified illustration, and all the analysis is carried out in the sagittal plane.

We associate the periodic gait of an actuated bipedal robot to a limit cycle behavior of the piece-wise continuous non-linear system represented by the dynamics in single support and double support. With the help of a phase portrait of a global variable, the existence of a limit cycle and its convergence, i.e. gait stability can be proved. The key point is to prove the contraction of the phase space volume as the system evolves in time. Noting that our robot has a phase space volume conserving Hamiltonian dynamics during the single support, we naturally search for the cause of the existence of limit cycle.

### 5.1 Contraction in switching control

In biped walking control, using the switching control as proposed in this paper, one active switching point is between a double support phase and a single support phase. Figure 11 shows a limit cycle of the bipedal walking robot. The shaded area indicates the contraction area or contraction volume. Because the dynamics in the double support phases and the dynamics of a swing leg in the single support phases are well controlled, in order for the phase trajectory to converge to a limit cycle, contraction tuning is required for the dynamics of a stance leg in single support.

Consider session  $t_1 - t_2$  in cycle  $(k+1)$  in Figure 7. Let

$$\Delta \mathbf{f}_{k+1}^{\&}(t_1) = \mathbf{f}_{k+1}^{\&}(t_1) - \mathbf{f}_k^{\&}(t_1) \quad (12)$$

The switching surface adjustment is defined as

$$S_{K+1}(t_1) = \Delta \mathbf{f}_{k+1}(t_1) - \mathbf{I} \cdot \Delta \mathbf{f}_{k+1}^{\&}(t_1) = 0 \quad (13)$$

where  $\mathbf{I} > 0$ .

The switching control at  $t_1$  is:

$$\Delta \mathbf{f}_{k+1}(t_1) = \mathbf{I} \cdot \Delta \mathbf{f}_{k+1}^{\&}(t_1) \quad (14)$$

$$\mathbf{f}_{k+1}(t_1) = \mathbf{f}_k(t_1) + \mathbf{I} \cdot \Delta \mathbf{f}_{k+1}^{\&}(t_1) \quad (15)$$

Assuming that angular position and velocity variations in the knee and hip joints of stance leg can be ignored during this period of time, the contraction property in time interval  $t_1 - t_2$  can be proved as below.

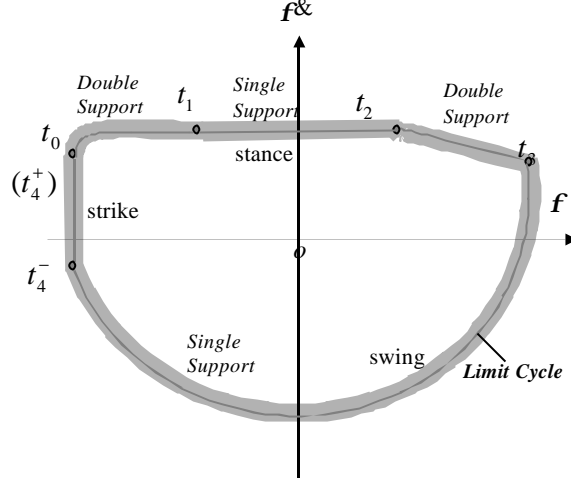


**Figure 11:** Contraction tuning by switching control. The shaded area represents the contraction volume.

The increment of kinetic energy at  $t_1$ ,  $t_2$ , and the increment of potential energy at  $t_1$  can be formulated as follows respectively,

$$\Delta E(t_1) = \frac{1}{2} ml^2 [\dot{\mathbf{f}}_{k+1}(t_1)^2 - \dot{\mathbf{f}}_k(t_1)^2] \quad (16)$$

$$\Delta E(t_2) = \frac{1}{2} ml^2 [\dot{\mathbf{f}}_{k+1}(t_2)^2 - \dot{\mathbf{f}}_k(t_2)^2] \quad (17)$$

$$\Delta P(t_1) = mgl[\cos(\mathbf{f}_{k+1}(t_1)) - \cos(\mathbf{f}_k(t_1))] \quad (18)$$

where  $m$  is the lumped mass of the biped, and  $l$  is the length from the COM of the biped body to the ankle joint of the stance leg.

Since the dynamic model of the stance leg can be approximately considered as an inverted pendulum, the dynamics of the biped are Hamiltonian in  $t_1 - t_2$ . Then,

$$\Delta E(t_1) + \Delta P(t_1) = \Delta E(t_2) \quad (19)$$

where  $\Delta P(t_2) = 0$  because the swing leg control ensures the same posture when striking the ground. From equations (15-19), we can derive

$$|\dot{\mathbf{f}}_{k+1}(t_2) - \dot{\mathbf{f}}_k(t_2)| \leq c_1 |\dot{\mathbf{f}}_{k+1}(t_1) - \dot{\mathbf{f}}_k(t_1)|, \quad (20)$$

where  $0 < c_1 < 1$ .

From the above inequality (20), the contraction property in session  $t_1 - t_2$  is proved. When the motion of the knee joint and hip joint of the stance leg cannot be ignored, the proof of contraction property, i.e. equation (20), can be done by means of a more complex dynamic model [15], which will be addressed in detail in a future paper.

With Figure 12, we can illustrate the above control effect more clearly. The dynamics of the robot in Figure 12 are Hamiltonian. By means of the above control (adjusting the switching angle), the kinetic energy will be balanced. Therefore, the phase trajectory will converge to the balanced energy state, i.e.  $\Delta E(t_2) = 0$ , where the limit cycle appears. Hence the phase trajectory will converge to the limit cycle session  $L(t_1, t_2)$  eventually by a series of switching control actions.

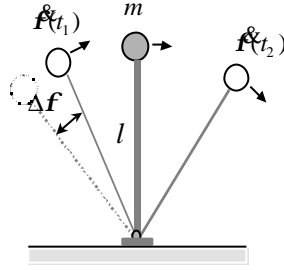


**Figure 12:** Dynamic model of the stance leg in the single support phase, where  $m$  is the mass and  $l$  is the length of the equivalent inverted pendulum.

Now we can prove the contraction property in session  $t_0 - t_1$ . Assume that virtual model control [10] is applied in the double support phase with the corresponding joint torques computed from the Jacobian (we can also prove the contraction property similarly if tracking control is used instead of virtual model control in this session). Then we have the following simplified lumped parameter dynamic model,

$$m\dot{v} = k_p (v_d - v) \quad (21)$$

where  $v$  represents the forward velocity of the biped,  $v_d$  is the desired forward velocity, and  $k_p$  is the control gain in the virtual space. Then the final velocity at the end of double support phase is,

$$\begin{aligned} v(t_1) &= v(t_0) + \frac{v_d k_p}{m} e^{-\frac{k_p}{m} t} \int_{t_0}^{t_1} e^{\frac{k_p}{m} w} dw \\ &= v_d + [v(t_0) - v_d] e^{-\frac{k_p}{m} t} \end{aligned} \quad (22)$$

where  $t = t_1 - t_0$  is the time interval for the double support phase.

Applying the above equation to cycle  $k$  and  $k+1$ , and plugging the geometric relation between  $v$  and  $\mathbf{f}$  in (21), we can derive

$$|\mathbf{f}_{k+1}(t_1) - \mathbf{f}_k(t_1)| \leq c_2 |\mathbf{f}_{k+1}(t_0) - \mathbf{f}_k(t_0)|, \quad (23)$$

where  $0 < c_2 < 1$ .

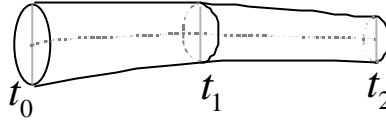


**Figure 13:** A diagram of contraction tuning.

Combining equation (20) and (23), we prove the contraction property in the session  $t_0 - t_2$  (see Figure 13). We can prove the contraction for session  $t_2 - t_3$  (a double support phase) the same way as we did with session  $t_0 - t_1$ . For session  $t_3 - t_4$  (a swing phase), trajectory control is used, and contraction is realized by tracking controllers. Therefore, the contraction is guaranteed for sessions  $t_0 - t_2$  and  $t_2 - t_4$  with the switching control and control sub-systems. The orbit of the global variable will approach the limit cycle. Hence the global gait stability is achieved. This proof can also be reformulated in the standard  $\mathbf{e} - \mathbf{d}$  argument in a mathematically rigorous form (as introduced in section 4.3).

## 6 Simulations and Discussion

We applied the switching control approach to a simulated 7-link planar bipedal walking robot (*Spring Flamingo*, a planar biped built by Jerry Pratt, MIT Leg Lab.; see Figure 14). The robot has a height of 1.2 meters, leg length 0.8 meters, foot length 0.18 meters, and body weight 13.5 kg. There are six joint actuators for the hip, knee and ankle in each leg. In our simulation, several control sub-systems have been designed for single support phases and double support phases. The proposed switching control was implemented and achieved stable locomotion for the planar bipedal walking robot.

Figures 15-17 below show the results from a six-second simulation. The simulation results show that the limit cycle was achieved very quickly. Hence a stable gait is also realized. Figure 15 shows the phase portrait of the global variable of the left leg. We observe that the walking gait converged to a limit cycle quickly. Figure 16 shows the phase portraits of hip, knee and ankle joints of the left leg. The behaviors of the right leg are similar. Figure 17 shows the data profile of joint angular positions and velocities of the left leg during the simulation of bipedal walking. A stick diagram (in Figure 18) shows that both the postural stability and gait stability are well maintained.

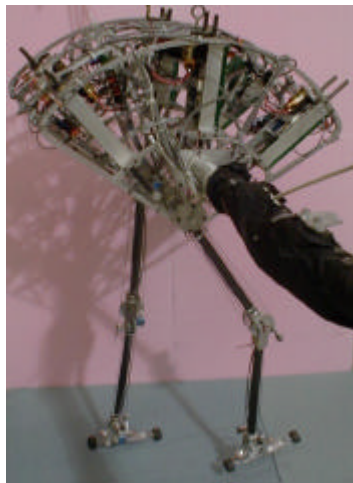
In the above switching control approach, bipedal gait stability is measured by means of two global gait variables. If the limit cycle of those global variables is reached, a periodic walking gait is realized for a bipedal walking robot. Provided that a proper height is well maintained during walking, constant step length will be assured. In practice, gait stability is measured mostly by step length and time duration of a step, i.e. the step period [1]. The measurement (or the index for gait stability) used in this study gives stronger conditions for gait stability.

## 7 Conclusion

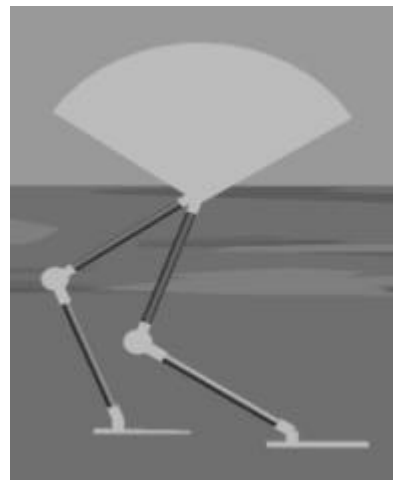
A nonlinear switching control approach was presented that achieved stable bipedal locomotion of a biped. With this control technique, one can obtain gait stability and postural stability. Gait stability was proved using nonlinear system theory.

Simulation results have shown the effectiveness of this switching control approach. The simulated planar bipedal walking robot achieved postural stability and gait stability.

This switching control approach can be applied to a 3-D humanoid walking robot. Currently, we are working on the control of a 3-D humanoid walking robot (called "M2") with a similar switching scheme.



(a)



(b)

**Figure 14:** Bipedal walking robot, *Spring Flamingo* (courtesy of Jerry Pratt). There are no arms, no vision system in this robot. (a) picture of the robot; (b) picture of the simulated robot.

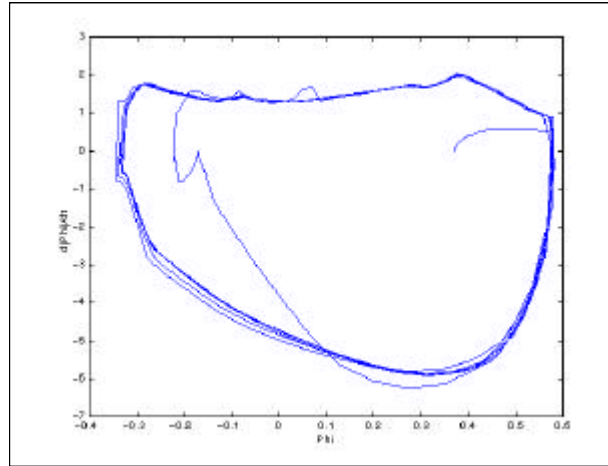


**Figure 15:** Simulation results of a planar biped robot. A phase plane diagram of global variable  $f$  (left leg) is shown. The dark line represents the limit cycle of the global variable.

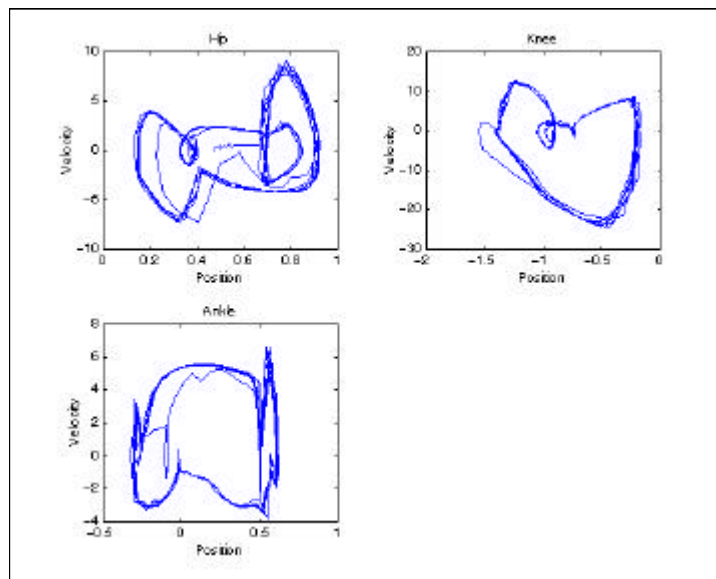


**Figure 16:** Phase plane portraits of hip, knee, and ankle joints of the left leg in the simulation.

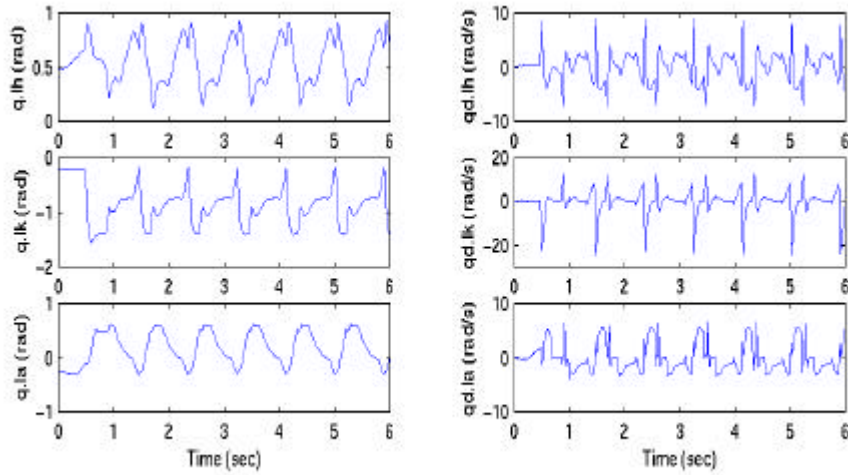


**Figure 17:** Simulation data profile of left leg joints. The responses in the left column ( $q.lh$ ,  $q.lk$ , and  $q.la$ ) are angular positions of hip, knee and ankle joints respectively. The responses in the right column ( $qd.lh$ ,  $qd.lk$  and  $qd.la$ ) are the angular velocities of hip, knee and ankle joints correspondingly. The periodic property is shown in the responses.

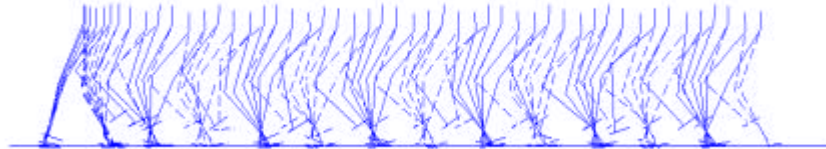


**Figure 18:** Stick diagram of bipedal walking. Solid lines are stick plots of the left leg and dashed lines are the stick plots of the right leg.

## Acknowledgements

The authors would like to thank Professor Alex Megretski, Professor Steve Massaquoi, and Bruce Deffenbaugh for constructive comments on the switching control theory and dynamic modeling, and Dr. Jerry Pratt for several discussions on the dynamics of bipedal walking robots.

## References

1. M. Vukobratovic, B. Borovac, D. Surla and D. Stokic, Bipedal Locomotion: Dynamics, Stability, Control and Application, *Scientific Fundamentals of Robotics 7*, Springer-Verlag, New York, 1990.
2. K. Hirai, M. Hirose, Y. Haikawa and T. Takenaka, The Development of Honda Humanoid Robot, *IEEE International Conference on Robotics & Automation*, Leuven, Belgium, May, 1998.
3. Q. Li, A. Takanish, and I. Kato, Learning Control of Compensative Trunk Motion for Biped Walking Robot Based on ZMP Stability Criterion, *IEEE/RSJ International Workshop on Intelligent Robots and Systems*, Raleigh, NC, 1992.
4. J. Hu, J. Pratt and G. Pratt, Adaptive Dynamic Control of a Bipedal Walking Robot with Radial Basis Function Neural Networks, *IEEE International Conference on Intelligent Robots and Systems*, Victoria, Canada, October, 1998.
5. J. Hu, M. Williamson, and G. Pratt, Bipedal Locomotion Control with Rhythmic Neural Oscillators, *IEEE International Conference on Intelligent Robots and Systems*, Kyongju, Korea, October, 1999.
6. G. Taga, A Model of the Neuro-musculo-skeletal System for Human Locomotion: I. Emergence of Basic gait, *Biological Cybernetics*, 73, 97-111, 1995.
7. A. Goswami, B. Espiau and A. Keramane, Limit Cycles and Their Stability in a Passive Biped Gait, *IEEE International Conference on Robotics & Automation*, Minneapolis, Minnesota, April, 1996.
8. H.K. Khalil, *Nonlinear Systems*, Prentice Hall, Upper Saddle River, NJ 07458, 1996.
9. T. McGeer, Passive Dynamic Walking, *International Journal of Robotics Research*, 9-2, pp.62-82, 1990.
10. J. Pratt, P. Dilworth and G. Pratt, Virtual Model Control of a Bipedal Walking Robot, *IEEE International Conference on Robotics & Automation*, New Mexico, April, 1997.
11. F.E. Lewis, C.T. Abdallah and D.M. Dawson, *Control of Robot Manipulators*, Macmillan, 1993.
12. H. Miura and I. Shimoyama, Dynamic Walk of a Biped, *International Journal of Robotics Research*, Vol. 3, No.2, Summer, 1984.
13. J.E. Slotine and W. Li, *Applied Nonlinear Control*, Englewood Cliffs, NJ: Prentice Hall, 1991.
14. J. Pratt and G. Pratt, Exploiting Natural Dynamics in the Control of a 3D Bipedal Walking Simulation, *International Conference on Climbing and Walking Robots (CLAWAR99)*, Portsmouth, UK, Sept., 1999.
15. J. Hu, Stable Locomotion Control of Bipedal Walking Robots: Synchronization with Neural Oscillators and Switching Control, Ph.D. Thesis, Dept. of Elec. Eng. & Computer Science, MIT, Cambridge, MA 02139. Expected in August 30, 2000.
16. J. Hu and G. Pratt, Stable Locomotion Control of a Bipedal Walking Robot by Means of Switching Control Theory, *Technical Report No. LL00101*, MIT Leg Lab., January, 2000.
17. A.F. Vakakis and J.W. Burdick, Chaotic Motions in the Dynamics of a Hopping Robot, *IEEE International Conference on Robotics & Automation*, Vol. 3, 1990.